Original Research Paper

Visible Derivative Spectroscopic Monitoring of the Old Woman Creek National Estuary During a Historically Dry Year and a Wet Year

[1]Lorita Nivanthi Mihindukulasooriya, [2]Brenna Shae Mabry, [3]Madison Slocum and [4]Joseph Daniel Ortiz

[1]*Department of Physics, Geology and Engineering Technology, Northern Kentucky University, Highland Heights, Kentucky, USA*
[2]*Midwestern Laboratories, Omaha. Nebraska, USA*
[3]*Raytown Quality Schools, Raytown, Missouri, USA*
[4]*Department of Earth Sciences, Kent State University, Kent, Ohio, USA*

Abstract: Visible derivative spectroscopy was used to interpret the sediment and phytoplankton assemblages within the old woman creek natural estuarine reserve during the summers of 2016 and 2017. A Varimax-rotated Principal Component Analysis (VPCA) of reflectance data collected from four sampling sites in 2016 identified three Varimax-rotated Principal Components (VPCs): Diatom + Illite (2016-VPC 1), Dinoflagellate Algae + Cyanobacteria + Cryptophytes (2016-VPC 2) and Cyanobacteria + Illite + Dinoflagellate Algae (2016-VPC 3). Four leading components were identified from the VPCA of 2017 data collected from six sampling sites. These include a diatom + green algae + cyanobacteria (2017-VPC 1), suspended clay (2017-VPC 2) and two dinoflagellate algae communities, each of which was associated with sediments and cyanobacteria (2017-VPC 3 and 4). Significant correlations between chlorophyll-a versus 2017-VPC 1 and 2017-VPC 2 versus total suspended solids confirm these PCs' applicability as proxies for algal abundance and suspended material/sediments, respectively. During the wet 2017 sampling period, when the mouth bar controlling the flow from the estuary to Lake Erie was open; diatom, cyanobacteria and green algae abundance in the estuary declined immediately after rainfall and increased within two to three days as the estuary recolonized with phytoplankton transported from upstream. The inflow of storm water increased the concentration of insoluble clay minerals within the estuary but declined within two to three days. Suspended sediments were transported into the lake through the estuary when the mouth bar was open. As the mouth bar progressively narrowed towards the end of the 2017 sampling period, the amount of algae and suspended material transported into the lake declined and was more concentrated in the upstream sampling sites. Observed temporal and spatial variation of sediments demonstrates the significance of the estuary environments as natural sediment retention structures.

Keywords: Visible Derivative Spectroscopy, Phytoplankton, Algal Blooms, Estuary

Introduction

Lake Erie is the fourth-largest lake in the United States and the eleventh-largest lake by surface area in the world. It provides drinking water for 11 million people and is a valuable resource for navigation, manufacturing, power production and recreation (Shear and Wittig, 1995). Eutrophication has been a recurring problem in Lake Erie since the early 1900s. Environmental regulations and community cleaning attempts resulted in improved lake conditions by the late 1970s (Michalak *et al*., 2013). However, the lake entered a period of re-eutrophication during the mid-1990s, with blooms of variable intensity occurring each year through the present. In 2011, approximately 20% of the lake was covered by a cyanobacterial harmful algal bloom (Cyano HAB) which

scored a ten on the bloom severity index; an index based on the amount of biomass during the peak 30 days of the bloom (Stumpf *et al.*, 2012). The bloom that developed in 2014 was less severe but disrupted the water supply to the city of Toledo (population of approximately 280,000) for three days due to its proximity to the water intake system. A record-breaking, severe bloom covered the lake in 2015, scoring 10.5 on the bloom severity index (Stumpf *et al.*, 2012). Although this bloom covered a lower surface area compared to 2011, the bloom's cyanobacterial density was higher compared to that of 2011. Eutrophication is severe in the western basin of Lake Erie where rivers drain from eight major watersheds, into Lake Erie. Old Woman Creek (OWC) is a relatively small watershed that drains to Lake Erie. The OWC Natural Estuarine Research Reserve (OWC-NERR) resides in a freshwater estuary that is directly connected to Lake Erie. Coastal wetlands such as those associated with OWC are critical to the health of Lake Erie by providing water quality enhancement, flood and erosion control and fish and wildlife habitat.

The OWC-NERR site is in a highly eutrophic estuary due to the surrounding area being mostly agricultural. The estuary accumulates significant amounts of sediment and nutrients from the watershed and seasonally serves as a sink for nutrients when the mouth is barred (Bernal and Mitsch, 2008). The influx of nutrients from the watershed and well-mixed water column stimulates phytoplankton production. Water levels across the estuary are frequently influenced by Lake Erie water levels and storm activity. Intermittently, the mouth bar closes due to the longshore current from Lake Erie, overwhelming the tributary flow (Wijekoon, 2007; Bonini, 2013; 2016). Water retention time within the estuary is usually less than a day when the mouth is open (Herdendorf *et al.*, 2004). As a result, nutrients and algal communities can be transported into Lake Erie. The formation of the mouth bar creates conditions that can transform contaminants or settle them to the bottom of the estuary. Hence, estuary water is cleansed as it slowly percolates through the mouth bar to Lake Erie (Herdendorf *et al.*, 2004).

Rapidly reproducing algae and cyanobacteria can form Cyanobacterial Harmful Algal Blooms (HABs) in lakes and ponds. Most of these HABs produce toxic compounds hazardous to human health, making water bodies incongruous for human consumption. Even non-toxic blooms can disrupt the ecological structure and degrade the aesthetic value of water bodies (Michalak *et al.*, 2013). Hence, frequent water quality monitoring programs are necessary to provide sufficient early warnings to the public. The algal bloom at OWC is generally not dominated by toxic cyanobacteria, so we refer to the impact of eutrophication here as "algal blooms" as opposed to Cyano HABs. Common methods of identifying and quantifying algal blooms include direct cell counts, High-Performance Liquid

Chromatography (HPLC) and quantitative, real-time PCR. Although these methods can provide a direct count of algal and cyanobacteria species or closely related proxies; they are expensive, time-consuming and require specifically trained personnel (Ortiz *et al.*, 2013). Hence, these methods cannot provide sufficient spatial and temporal coverage to continuously monitor the water quality in large water bodies in ways that are cost-effective. In contrast, Visible Derivative reflectance Spectroscopy (VDS) is a rapid, cost-effective approach to identifying color-producing agents in water, including phytoplankton and suspended minerals. Additionally, the direct in-situ chlorophyll measuring methods only gives a quantitative estimate of chlorophyll and phycocyanin in water. In contrast, the VDS method based on color reflectance provides a comprehensive qualitative estimate of other major pigments as well as sediments present in the water. Fine sediments often degrade aquatic habitats creating hypoxia and transporting pollutants (Walling, 2013). Hence identifying sediment composition can be useful in tracing the source of fine sediment when implementing sediment control measures (Walling, 2013).

The present work demonstrates the applicability of VDS on a small wetland setting to identify the composition of phytoplankton communities and suspended sediments. Old woman creek estuary provides an ideal setting for algal bloom studies as it directly affects the water quality of Lake Erie. Moreover, the shallowness of the estuary provides an excellent setting for field studies without the need for expensive research vessels. Additionally, the study of spatial variability of algae and sediment composition in OWC will help us to evaluate the conditions of lake Erie's coastal wetlands. We hypothesized that the comparison of data collected during the summer of 2016 versus the summer of 2017 will allow us to understand the temporal variation of water quality at the OWC estuary and Lake Erie. Additionally, the comparison of spectroscopic data from the two summer monitoring periods will allow us to understand the differences in algal and sediment compositions under two different hydrological conditions: Open versus closed mouth bar. Furthermore, a comparison of summer 2017 reflectance data with algal cell counts and chlorophyll concentrations measured from a YSI-EXO2 sonde (fluorometrically) is provided to understand the strengths and limitations of each method.

Materials and Methods

Study Area

OWC-NERR is located approximately 5 km (3 mi) east of Huron, Ohio. This site is one of the few natural estuaries left in the south-central region of Lake Erie, as much of the estuaries around Lake Erie have been drained or artificially diked (Mitsch and Reeder, 1992). OWC drains approximately 69 km^2 (27 mi^2) of a primarily agricultural watershed (Herdendorf *et al.*, 2004;

Mitsch and Reeder, 1992). The estuary consists of the lower 2.1 km (1.3 mi) of the creek that drains into the central basin of Lake Erie. The widest portion of the estuary is 0.34 km (0.21 mi). Water levels within the lower estuary are usually less than one meter, except near the mouth where depths can reach up to two meters (Klarer and Millie, 1989). Shallower depths are often dominated by common reeds (*Phragmites australis*), while aquatic vegetation such as water lilies (*Nymphaea tuberosa*) and water lotus (*Nelumbo lutea*) tend to dominate deeper depths, increasing in coverage as the seasons progress from spring to summer (Bernal and Mitsch, 2008). Phytoplankton populations, which seem to be storm-regulated (Klarer and Millie, 1989), dominate the open water, which is rich in sediment from wind mixing and the mating and feeding behavior of invasive carp (*Hypophthalmichthys molitrix* and *H. nobilis* that grow to 27-54 kg (or 60-120 lbs).

OWC is classified under the temperate-humid continental-long summer climate (Herdendorf *et al*., 2004). Four distinct seasons prevail in the region with large seasonal temperature ranges (Herdendorf *et al*., 2004). Due to the proximity to Lake Erie, winds from the northerly quadrants tend to lower the daily temperatures in the summer while raising them in the winter (Herdendorf *et al*., 2004). As is typical of a continental climate, the region's precipitation is highly variable on a yearly basis (Herdendorf *et al*., 2004). However, precipitation in the OWC watershed is typically abundant and evenly distributed with autumn being the driest season (Herdendorf *et al*., 2004). The average annual precipitation is approximately 89 cm (35 in) with winds averaging 10 km/h (6 miles/h) in summer and 14 km/h (8.7 miles/h) in winter (Herdendorf *et al*., 2004). Though these prevailing winds are southwesterly, the southern coast of Lake Erie is affected by severe storm systems from the north that can cause extensive damage to and recession of the shoreline. On average, there are 12 weather disturbances a week that affect the watershed, which can cause sudden fluctuations in temperature, wind direction and precipitation (Herdendorf *et al*., 2004).

The orientation of Lake Erie parallels the prevailing wind direction causing the most common seiche to be longitudinal. Formation of the mouth bar is caused by longshore currents that arise from geostrophic balance (Herdendorf *et al*., 2004). The hydrology of the estuary is greatly influenced by the presence of the mouth bar. During the summer and winter, the mouth is barred for extended periods. As water levels rise in the spring and fall, or during severe storm events, the mouth bar is breached (Herdendorf *et al*., 2004). This generalized pattern can be disrupted by various meteorological events. Storm pulses from the watershed can cause the estuary to flood, breaching the mouth bar (Herdendorf *et al*., 2004). On average, there is more than one storm per month causing the mouth bar to be open for much of the year,

which occur with stochastic frequency. Due to the shallowness of the estuary and the similar elevation of the estuary and the mean lake level, even minor fluctuations in lake levels can cause significant effects on the estuary (Herdendorf *et al*., 2004). Daily changes in estuary water levels caused by seiches from Lake Erie range from 0.1-0.2 m (Herdendorf *et al*., 2004). However, storm activity can cause changes as much as 1-2 m (Klarer and Millie, 1989). In addition to water level changes, seiches can lead to chemical exchange between the estuary and the lake (McCarthy *et al*., 2007).

Three significant sources of sediment in the creek have been identified: Glacial till plains in the upper drainage basin, exposed bedrock in the central reach of the OWC basin (Ohio Shale, Bedford Shale and Berea Sandstone) and glacial-lacustrine deposits in the lower OWC basin (Evans and Seamon, 1997). The soil has been classified as Adrian muck by the natural resource conservation services, corresponding to outwash plains and former bogs (Bernal and Mitsch, 2008). The substrate of the estuary is almost entirely silty-clay (Klarer, 1988) and consists mostly of quartz, illite and chlorite (Buchanan, 1983). The silty nature of the soil and sediment, as well as a well-mixed water column, causes the lower estuary to be turbid throughout most of the year (Herdendorf *et al*., 2004).

Field Methods

Water samples were collected daily over a ten-day period to measure reflectance and Total Suspended Sediments (TSS) during the summer of 2016 and 2017 (25/07/2016 to 04/08/2016, 11/07/2017 to 20/07/2017). Four sites were sampled (OL-overlook, WM-wetland mouth, MO-mouth bar, VC-vegetated channel; Fig. 1) during the summer of 2016, while two additional sites were sampled during the summer of 2017 (ex-excess phytoplankton growth and Erie-MO-nearshore Lake Erie adjacent to the mouth bar). Sites OL, WM and EX are located south of the US Route 6 bridge, while MO and VC are located north (downstream) of the bridge. OL is located furthest upstream from the mouth bar. WM is on the opposite side of the estuary from OL, close to the west bank of OWC. Sites OL and WM are two sites that are continuously monitored by the national estuarine research reserve System Wide Monitoring Project (SWMP). Site EX is located close to the east bank of OWC, opposite from the site WM and downstream from OL and had a significant algal concentration during both sampling years. Site VC is located among an extensive zone of American water lotus (*Nelumbo lutea*), downstream of the route 6 Bridge. Site MO is located closest to the mouth bar within the estuary. The first five sampling sites are located within the estuary and are accessible by canoe or rowboat. Site Erie-MO is located in the nearshore zone of

Lake Erie, approximately 5 m from the mouth bar and is accessible by wading. The mouth bar was closed during the summer 2016 sampling period, but was open during the summer 2017 sampling period, allowing a comparison of conditions during these two system states. Table 1 summarizes the analysis conducted at different sampling sites during the two sampling years.

In 2016, water quality parameters for the sampling sites were measured on the last day of sampling (04/08/2016) using a multi-parameter hydro lab sonde, while these properties were measured daily in 2017. During both sampling periods, GPS coordinates were recorded for each site and PVC pipes with research tags were placed as visual markers at each site to ensure consistent sampling. The canoe or rowboat was anchored or tethered to the vertical pole placed as part of the SWMP system to conduct fieldwork. At each site, a Secchi depth was recorded to measure turbidity, with the exception of the Erie-MO site due to wave action. Water temperature, pH, conductivity, salinity and Total Dissolved Solids (TDS) were measured daily using Oakton PCS Testr 35™, while Oxidation-Reduction Potential (ORP) was measured using Oakton ORP Testr 10™. Surface water samples were collected into Nalgene bottles at five sites located within the estuary (WM, MO, EX, VC and OL) over five days during the 2017 sampling period (11/07/2017 to 15/07/2017), for algal cell counts. Bottles were rinsed at each site with source water before sampling. Samples were preserved by adding 7.5 mL of 1% Lugol's iodine per 250 mL of the sample and were stored and transported at 4°C until use in the lab.

Laboratory Methods

A multi-parameter YSI sonde was used to measure chlorophyll concentration during the last six days of sampling in the summer of 2017 (15/07/2017 to 20/07/2017). Unfiltered 500 mL samples were mixed thoroughly before using the probe. The chlorophyll probe automatically determines the chlorophyll-a concentration based on the fluorescence. Three measurements were taken every other minute from each. The average from three measurements was used for analysis.

Visible Derivative Spectroscopy (VDS) and Total Suspended Solids (TSS)

Plant pigments, their degradation products, oxides, siliciclastic and carbonate minerals associated with suspended sediment have unique combinations of wavelengths at which they absorb and scatter UV/visible and Near-Infrared (NIR) radiation. Visible reflectance spectroscopy involves measuring the inverse of the absorption spectra, if contributions from backscatter are negligible ($R_{rs} \sim= b_b/(a+b_b)$), where R_{rs} is remote sensing reflectance, b_b is particle backscatter and a is absorption following, Gordon *et al.*, (1975; 1988). The derivative transformation of reflectance data minimizes the scattering effect of radiatio. This data can then be compared with the reflectance spectra of known minerals (similar to the spectral matching method used in XRD) to identify and quantify the composition of suspended sediments. Similarly, the phytoplankton composition in water can be identified by comparing the reflectance signal of water with that of known photosynthetic pigments. The method has been successfully applied to estimate algal chlorophyll concentration and suspended sediment compositions in lake sediment, freshwater and marine ecosystems as well as to estimate algal and cyanobacterial biomass from multispectral and hyperspectral images (Han, 2005; Ortiz *et al.*, 2013; 2019 Mihindukulasooriya *et al.*, 2015; Avouris and Ortiz, 2019). The method had also been successfully used to extract color-producing agents from four hyperspectral HSI12 swaths flown over the western basin of Lake Erie. Ortiz *et al.* (2017) used the method to extract information about the color-producing agents along the southern shore of the Central Basin of Lake Erie. Spectral decomposition of hyperspectral data (over 400-900 nm) yielded six components explaining 92.8-97.4% of the variance, with the leading component comparable to the spatial pattern of the National Oceanic and aeronautical administration cyanobacterial index (Ortiz *et al.*, 2017). A comparison of hyperspectral data calibrated using several different atmospheric correction methods including the spectral decomposition method confirms that the method is insensitive to the background noise and hence is an effective method to quantify (Ortiz *et al.*, 2017).

250 mL of collected water samples were filtered through 0.4 μm GF/F filter papers shortly after sampling using a 16-psi vacuum pump at the OWC national estuarine research laboratory. Bottles were mixed thoroughly before filtering and the filter papers were handled with metal forceps to prevent contamination. The filters were oven dried for 24 h at 60°C. The filters were weighed before filtration and after drying. Total Suspended Solids (TSS) were calculated for each sample by subtracting the post-dried filter weight from the pre-dried filter weight. The resulting weight was divided by 250 and multiplied by 1000 to convert the weights to mg/L.

Color reflectance was measured on the oven-dried filter papers using a Konica-Minolta CM-2600D spectrophotometer. The Konica-Minolta CM-2600D spectrophotometer measures the reflectance at 10 nm intervals from 360-740 nm. The device was allowed to warm up for 30 min before taking measurements.

Table 1: Summary of methods conducted at different sampling sites during the two sampling years

Year/-dates Site	Reflectance followed by VPCA		TSS		Algal cell counts	Chlorophyll-a (fluorometric)	In-situ water quality	
	2016 07/25-08/04	2017 07/11-07/20	2016 07/25-08/04	2017 11/07-20/07	2017 07/11-07/15	2017 07/15-07/20	2016 08/04	2017 07/11-07/20
OL	✓	✓	✓	✓	✓	✓	✓	✓
WM	✓	✓	✓	✓	✓	✓	✓	✓
VC	✓	✓	✓	✓	✓	✓	✓	✓
MO	✓	✓	✓	✓	✓	✓	✓	✓
EX		✓		✓	✓	✓		✓
Erie-MO		✓		✓		✓		✓

The filters were covered with Glad™ plastic wrap to avoid direct contact with the integration sphere and potential contamination.

The Konica-Minolta CM-2600D spectrophotometer was calibrated between each sample using a black light trap and a calibrated white reference standard. As a control, three white measurements were taken between each sample. The filters were divided into four quadrants and a measurement was taken at each quadrant. The average from the four quadrants was used as the reflectance from each sample. Spectral data were exported to a computer through SpectraMagic™ software for data analysis.

Algal Cell Counts

Water samples preserved in 7.5 mL of 1% Lugol's Iodine were used for algal cell counts. Samples were processed and counted according to a protocol adapted from (Brierley *et al*., 2007). Briefly, samples were removed from 4°C storage and were mixed for 2 min using gentle inversions of the bottle. 1 mL of the sample was transferred to a graduated cylinder and diluted 1:10 using 1× Phosphate Buffered Saline (PBS). The diluted samples were allowed to settle in an Utermöhl counting chamber (aquatic research instruments; Hope, Idaho) for approximately 24 h before counting. The counting chambers were carefully placed under an inverted microscope at the end of the settlement period and the cells were counted at 400× magnification. Class-level identifications were made for each algal cell and cyanobacteria were identified at the Phylum level. Cells were counted across horizontal transects until 100 units of the most abundant groups were counted. The relative percentage for each taxon was calculated using the formula; relative percentage = (number of cells from each taxon/total number of phytoplankton cells counted) *100.

The relative abundance of each phytoplankton group was compared to VPC data at each individual site.

Theory and Calculations

First derivative spectra of visible reflectance data (dR/λ; rate of change of reflectance as a function of wavelength) were calculated to minimize noise and the effects of scattering. The KSU spectral decomposition method, a Varimax-rotated, Principal Component Analysis (VPCA) was conducted on the centered first derivative spectra using SPSS™ to extract the principal components. Two separate VPCAs were conducted for the years 2016 and 2017 due to the difference in the mouth bar conditions and the number of sampling sites between the two sampling years. Extracted components were compared using stepwise multiple regression against a published database of mineral and pigment reflectance spectra compiled by the United States Geological Survey (USGS) spectral library (Clark *et al*., 2007; Kokaly *et al*., 2017) or measured in the lab (Ortiz *et al*., 2009; 2019 Ortiz, 2011; Bouchard *et al*., 2013; Avouris and Ortiz, 2019). The component scores and the reference spectra were standardized to obtain a better fit. Stepwise linear regressions were performed using JMP ™ 5.0.1 to find the coefficients of each contributing pigment and/or mineral combination that were present at each time and location. The spectral library contains the reflectance spectra of 27 common individual photosynthetic pigments like chlorophyll-a and carotenoids, six pigment degradation products (e.g., phaeophytin-a) and total spectral reflectance signals from nine individual taxonomic divisions (Chlorophyta, cyanophyta) or classes (e.g., bacillariophyceae, Chlorophyceae) (Avouris and Ortiz, 2019). In the former case, the presence of a certain pigment in the reflectance signal is considered the presence of phytoplankton groups comprising the pigment, while in the latter case, the correlation to the individual division or class implies the presence of phytoplankton belonging to the said taxonomic category.

In order to understand the factors affecting algal blooms, VPCs were compared with measured water quality parameters and weather data. Weather data were downloaded from the NOAA national estuarine research reserve system's centralized data management website, which displays data collected from the SWMP sensors in OWC (https://cdmo.baruch.sc.edu//dges/). OWC discharge data was downloaded from the USGS water database (https://waterdata.usgs.gov/nwis/sw), for station number 04199155, old woman creek at berlin road near huron, ohio. The total precipitation for each day was calculated by adding the recorded precipitation within 24 h prior to the sampling time. Pearson's product-moment correlation coefficients (r-values) and the p-values were calculated using EXCEL™. The p-values of the correlations were determined using t-statistics. Correlations were conducted against parameters within each site as well as between individual sites to find any correlations between sampling sites.

Surface maps were prepared to understand the distribution and transportation of phytoplankton and sediment within the estuary using the leading two varimax-rotated scores from the six sampling sites for the sampling year 2017. A digital map of the estuary was prepared by digitizing satellite imagery of the OWC lower estuary. Surface concentration maps were prepared for each day by interpolating the values in between the discrete sampling sites using the Interpolation tool in ArcMap 10.3™. Values between the sampling sites were interpolated using spherical kriging, assuming that the width of the mouth bar was constant throughout the sampling period.

Results

Water quality data from 2016: Closed mouth bar conditions. Water quality parameters measured on the last-of-day sampling in the year 2016 are listed in Table 2. The temperature varied from 26.5-27.5°C, with the highest temperature at the Mouth bar (MO) and the lowest temperature at OL. The observed pH values varied between 7.18 and 7.35 with the lowest pH at the upstream OL location and the highest pH at MO. Similarly, specific conductivity increased from 546 μS at the upstream OL site to 549.7 μS at the downstream MO site. The mean air temperature and the cumulative precipitation during the sampling period (July 24th to August 4th) were 23.95°C and 26.5 mm respectively. The mean monthly temperature (July 5th to August 5th) and the cumulative monthly precipitation were 24.34°C and 68 mm respectively. USGS discharge of the old woman creek at Berlin road during the sampling period remained lower than the thirty-year mean discharge for the gauging station (USGS, 2017) except on July 25th. Discharge varied between 0.0249 m^3/s (0.88 ft3/s) to 0.0031 m^3/s (0.11 ft3/s) while the gauge height varied from 0.44 m (1.43 ft) to 0.36 m (1.19 ft). Peak discharge of 0.0249 m^3/s (0.88 ft3/s) was recorded on July 24th, fourteen hours prior to the first sampling date.

Water quality data from 2017: Open mouth bar conditions the range of values for water quality parameters during the 2017 sampling period and their averages are listed in Table 3. The average water temperature varied between 24.4-24.8°C with the lowest average temperature at the Nearshore Lake Erie site (Erie-MO, Table 3). The water was slightly alkaline with the average pH values varying between 7.9 and 8.4, with the highest pH at Erie-MO and lowest at OL. Both pH and temperature increased towards the mouth of the estuary. Average conductivity varied from 299-345 μS, with the lowest values at Erie-MO and highest at OL (most upstream site). This pattern is consistent with the spatial variation of conductivity during the summer of 2016. Average TDS and salinity varied from 212-245 and 144-166 ppm respectively, with the highest values at OL and lowest values at Erie-MO. Similarly, TSS decreased downstream from an average value of 32 mg/L at OL to 16.6 mg/L at the Lake. In summary conductivity, salinity, TDS and TSS decreased from upstream to downstream while pH and temperature increased downstream.

Table 2: Range of water quality parameters recorded during the 2016 sampling period

	MO	VC	WM	OL
Temperature °C	027.51	026.78	026.70	026.55
pH	007.36	007.22	007.19	007.18
ORP (mV)	437.62	433.33	434.82	415.79
Conductivity (μS)	549.77	549.53	549.47	546.00
TDS (ppt)	000.40	000.40	000.40	000.30
Salinity (ppt)	000.28	000.28	000.28	000.28
DO (%)	062.28	032.74	024.68	023.77
DO (mg/L)	004.09	002.18	001.64	001.59
Chlorophyll (μg/l)	023.71	027.25	030.21	036.80

Table 3: Range of water quality parameters and their mean values during the 2017 sampling period. The first number in each row represents the range of recorded values and the second number represents the average of the measured value during the ten-day sampling period

Sampling site	Erie/MO	MO	VC	EX	WM	OL
Temperature °C	23.4-25.4	23.5-27.10	23.2-27.00	23.0-27.00	22.5-26.9	22.8-27.00
	24.36	24.75	24.64	24.74	24.56	24.57
Secchi depth (in)	N/A	6.5-34.00	6.0-21.00	5.0-21.00	5.0-20.0	5.0-25.0
		19.10	14.70	13.40	14.10	13.80
pH	7.78-8.94	7.46-8.65	7.43-8.45	7.58-8.78	7.42-8.47	7.40-8.430
	8.46	8.10	7.90	8.00	8.00	7.90
ORP (mV)	195-243	196-248	197-246	191-241	181-265	197-268
	213.900	224.100	217.50	217.400	198.900	215.400
Conductivity (µS)	285-329	283-389	289-373	287-392	289-395	292-400
	299.300	325.700	327.90	337.800	335.600	345.000
TDS (ppm)	202-233	201-276	206-265	204-278	205-280	207-284
	212.300	231.500	233.100	239.200	238.300	244.700
Salinity (ppm)	137-158	136-188	140-180	139-189	140-191	141-193
	144.200	157.400	158.300	162.600	161.800	166.300
DO (%)	71.5-97.80	76.1-97.6	68.4-93.70	71.3-104.0	73.4-94.6	66.0-101.8
	89.81	87.90	78.07	88.02	82.40	85.04
DO (mg/L)	5.9-8.8	6.6-8.5	5.9-8.3	6.5-8.6	6.1-8.5	6.1-9.0
	7.91	7.67	6.85	7.770	7.300	7.48
Chlorophyll (µg/l)	5.7-12.9	5.8-35.30	4.7-23.3	4.7-39.10	4.8-34.	7.1-51.5
	8.22	15.63	12.650	17.98	16.56	19.13

The cumulative precipitation during 2017 was much higher compared to 2016, with a cumulative rainfall of 61.2 mm during the sampling period (July 10-20th) and 117.9 mm during the 30-day period from July 5th-August 5th. As a result of the higher precipitation, the discharge remained higher than the thirty-year mean discharge throughout the 2017 sampling period. The discharge varied between 19.68 m³/s (695 ft³/s) to 0.088 m³/s (3.11 ft³/s), while the gauge height varied from 2.8 m (9.3 ft) to 0.95 m (3.11 ft). Historically high discharges of 19.68, 8.13 and 7.31 m³/s (695, 287 and 258 ft³/s) were recorded on July 10th (10 h prior to the first sampling date), 12th (second day of sampling) and 13th (third day of sampling), respectively. The highest discharge in 2017 (19.68 m³/s) was approximately 800 times higher than the highest discharge in 2016 (0.0249 m³/s), while the gauge height was six times higher. The air temperature was slightly lower compared to 2016, with a 10-day mean temperature of 23.2°C during the sampling period and a 30-day (July 5th to August 5th) mean temperature of 23.33°C.

SI Table 1 lists the significant correlations observed between water quality parameters and their significant levels during the two sampling years.

Visible Derivative Reflectance

Center-weighted derivatives of the reflectance data from 2016 yielded three components (hereafter referred to as 2016 VPC 1, 2 and 3) explaining 95% of the variance in the data (Table 4). 2016-VPC 1 explains 65% of the variance and consists of Bacillariophycea (diatoms) and illite + kaolinites (Fig. 2a and 1, Tables 3-5. The second component (2016-VPC 2) explains 23% of the variance and is defined as a mixture of allophyocyanin, Chlorophycea (green algae) and phycoerythrin (Fig. 2b, Tables 2-3).

The third component of 2016 reflectance data (2016-VPC 3) explains 5.7 % of the variance and is a mixture of illite, peridinin (dinoflagellate algae pigment) and cyanobacteria (Fig. 2c, Tables 2-3).

Figure 3 demonstrates the temporal variation of these VPCs during the ten-day sampling period in 2016. Application of each of these VPCs as phytoplankton and/or sediment proxy is explained in the discussion.

The first four VPCs of the 2017 reflectance data explained 99% variance of the data (hereafter referred to as 2017 VPC 1, 2, 3 and 4). Each VPC correlates with corresponding mixtures of algal communities and/or suspended sediments listed in Tables 6-7. Temporal variation of these VPCs during the 2017 sampling period is demonstrated in Fig. 5. Increase in the 2017-VPC 1 score was observed towards the end of the sampling period at all sampling sites. Chlorophyll concentration follows a similar trend to VPC 1 at all six sampling sites (Fig. 6a).

Table 5: ANOVA for the pigment and/or mineral combinations for 2016 VPCs. Negative coefficients suggest an inverse correlation between the VPC and the variable

VPC	Variables	Coefficients	Standard error	T-test	P-value
VPC 1	Bacillariophyc eae Illite + kaolinite	0.84	0.080	9.35	5.8×10^{-10}
		0.36	0.080	5.17	1.9×10^{-5}
VPC 2	Phycoerythrin allophycocyani chlorophyceae	0.37	0.098	3.81	7.3×10^{-4}
		-0.59	0.095	-6.14	1.4×10^{-6}
		-0.46	0.098	-4.69	6.9×10^{-5}
VPC 3	Illite peridinin cyanobacteria	0.61	0.080	7.70	2.7×10^{-8}
		-0.43	0.080	-5.37	1.1×10^{-5}
		-0.26	0.080	-3.39	2.2×10^{-3}

Table 6: Regression statistics for 2017 VPCs and their correlated pigment and/or sediment assemblages

Total variance explained by the VPC	VPC 1	VPC 2	VPC 3	VPC 4
	50.8 %	37.8 %	9.5 %	0.98 %
Spectral pattern	Chlorophyceae + cyanobacteria + Bacillariophyceae	Smectite + chlorite	Myxoxanthophyll + Peridinin + goethite	Dinophyta + cyanophyta + calcite
Multiple R	0.88	0.95	0.74	0.92
R square	0.78	0.90	0.54	0.85
Adjusted R square	0.75	0.90	0.49	0.83
Standard error	0.32	0.32	0.73	0.42
F	31.65	274.96	10.64	50.25
Significance F	5.47898×10^{-9}	2.46157×10^{-16}	8.58242×10^{-5}	3.52477×10^{-11}

Table 7: ANOVA for the pigment and/or mineral combinations for 2017 VPCs. Negative coefficients suggest an inverse correlation between the VPC and the variable

VPC	Variables	Coefficients	Standard error	T-test	P-value
VPC 1	Chlorophyceae	-0.32	0.12	-2.65	0.01
	Bacillariophyceae	-0.13	0.11	-1.25	0.22
	Cyanobacteria	-0.15	0.10	-1.49	0.15
VPC 2	Smectite + chlorite	0.95	0.06	16.58	2.46157E-16
VPC 3	Myxoxanthophyll	0.12	0.21	0.58	0.566
	Peridinin goethite	0.36	0.20	1.80	0.083
		7.06	2.75	2.57	0.016
VPC 4	Dinophyta cyanophyta	-0.38	0.14	-2.77	0.0099
	Calcite	-0.22	0.13	-1.71	0.0996
		0.49	0.09	5.75	4.05×10^{-6}

In contrast to the increasing trend demonstrated by 2017-VPC 1, 2017-VPC 2 and 3 follow decreasing trends at the ERIE-MO site. A decreasing trend is demonstrated by 2017-VPC 2 at all the other sampling sites during the first 4 to 5 days of sampling and then shifts to an increasing trend.

Algal Cell Counts

Phytoplankton cell counts from the collected samples were categorized into 12 major classes. However, only four classes were present in the collected samples (SI Table 2). The dominant class of phytoplankton was Cyanophyceae, contributing to 74 to 96% of the cell counts. Presence of Cyanobacteria in two out of the three reflectance VPCs, further supports this observation. The relative abundance of Chlorophyceae varied between 2-6%, while 1 to 5% of the cell counts consisted of Bacillariophyceae or Euglenophyceae. Cryptophyceae (cryptomonads) were present only at one sampling site (WM) with 1 to 3% abundance. The highest phytoplankton diversity was observed at the site WM with, 74-90% Cyanophyceae, 3-6% Chlorophyceae, 4-6% Bacillariophyceae, 2-12% Euglenophyceae and 1-4% Cryptophyceae.
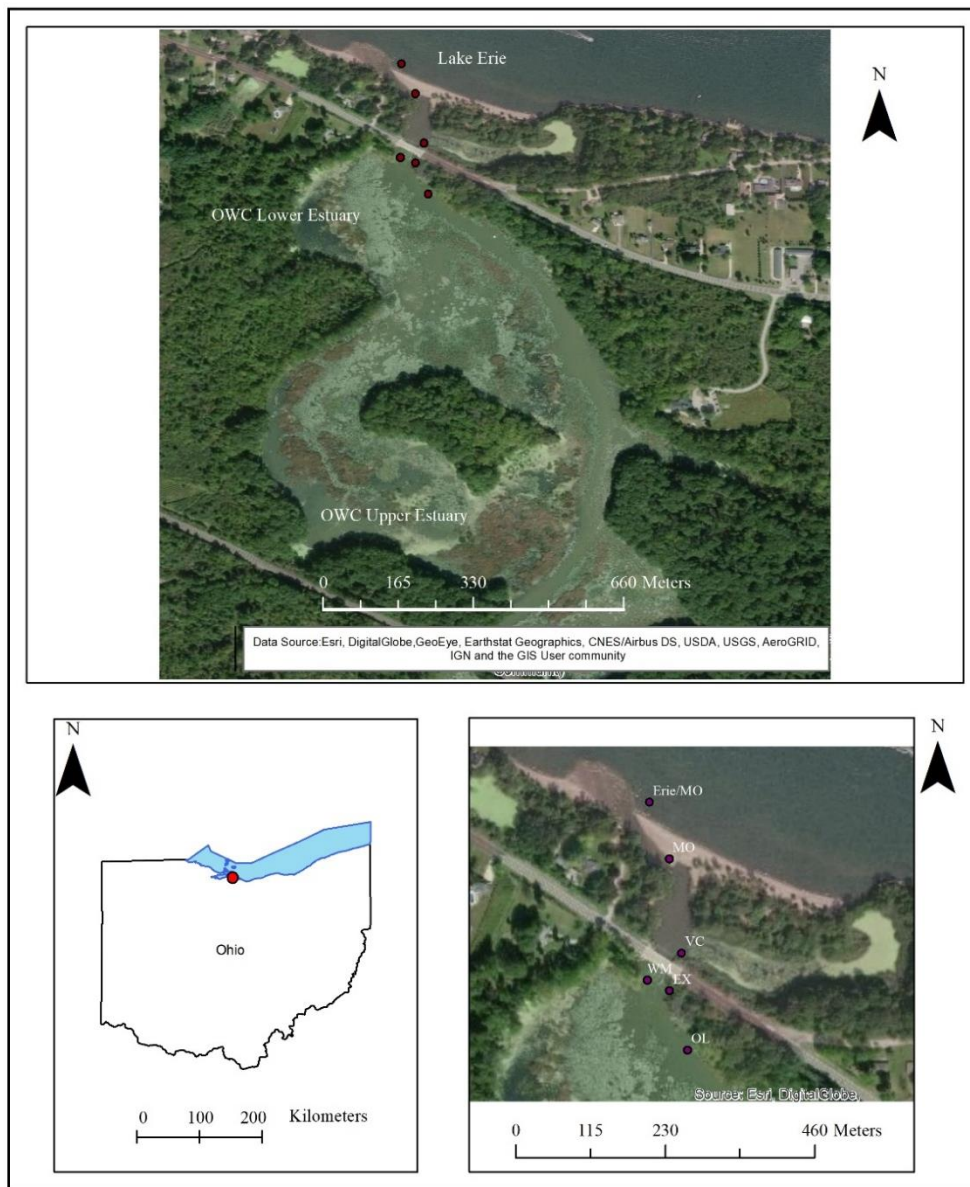
Fig. 1: Map of the Old Woman Creek Estuary showing the sampling sites (top) and the location of the estuary (colored circle) within the state of Ohio (bottom left) and the six sampling locations in the lower estuary (bottom right)
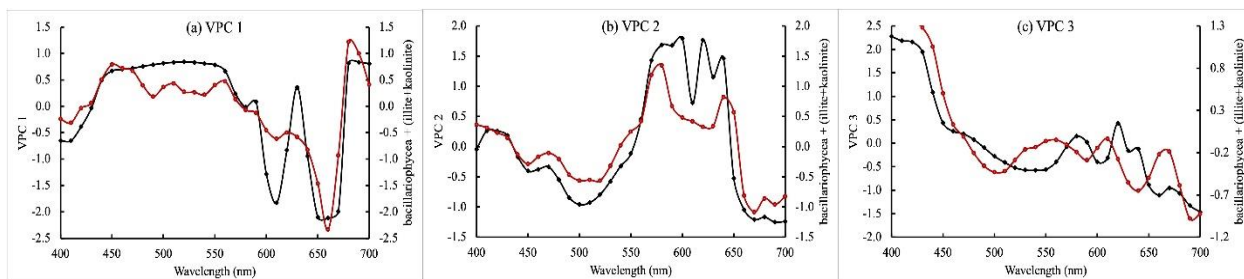

Fig. 2: Comparison of the first three principal components of summer 2016 VDS data with their reference spectra. The black line represents the VPCs and the red line represents their reference spectra
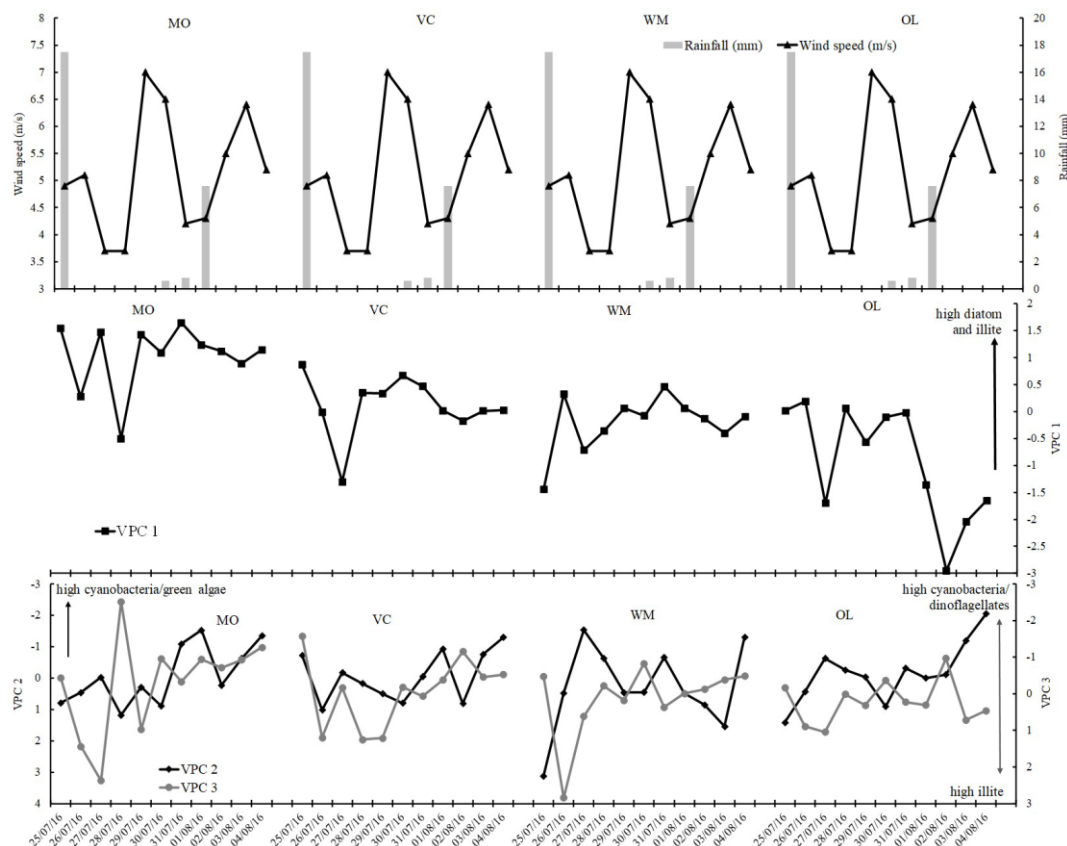
Fig. 3: Temporal variation of VPCs during the 2016 sampling year, the x-axis represents the sampling dates from 7/26/16 to 8/04/16, the black line and triangles in the top panel represent the maximum wind speed (m/s) during the time of sampling and the gray bars represent cumulative daily rainfall (mm)

Discussion

The leading VCP from 2016 (2016 VPC 1) is considered a proxy for diatoms and suspended sediments (Fig. 2a, Tables 3-4). The positive correlation between Bacillariophyceae, illite and kaolinite and 2016-VPC 1 indicates a higher diatom and illite + kaolinite abundance with high VPC scores. The second component (2016-VPC 2) correlates with allophyocyanin, Chlorophycea and phycoerythrin (Fig. 2b, Tables 2-3). Phycoerythrin and allophycocyanin are light-harvesting accessory pigments common in cyanobacteria, red algae and cryptophytes (Lemasson *et al*., 1973). As there have been no planktonic red algae identified in the OWC (Herdendorf *et al*., 2004), this component most likely represents the presence of cyanobacteria and cryptophytes. Cryptophytes are considered to be a common planktonic group at OWC and Lake Erie (Herdendorf *et al*., 2004; McCarthy *et al*., 2007). Allophycocyanin and Chlorophyceae negatively correlate with 2016-VPC 2, while phycoerythrin positively correlates with 2016-VPC 2. The negative correlation indicates a low abundance of green algae (Chlorophyceae) and cyanobacteria with high 2016-VPC 2 scores and vice versa.

In contrast higher abundance of Cryptophytes would be represented by higher 2016-VPC- 2 scores. The third component of 2016 reflectance data (2016-VPC-3) is considered a proxy for cyanobacteria + dinoflagellate algae and illite. Illite positively correlates with 2016-VPC 3, while peridinin and cyanobacteria negatively correlate with VPC 3, indicating lower cyanobacteria and dinoflagellate algae abundance with increasing illite concentration.

The leading principal component (2017-VPC 1) explains 50.8% of the variance and correlates with a mixture of Chlorophyceae (green algae), Bacillariophyceae (diatoms) and cyanobacteria (Tables 6-7 and Fig. 4a). Hence this VPC is considered a proxy for green algae, diatom and cyanobacteria abundance. Chlorophyceae, Bacillariophyceae and cyanobacteria negatively correlate with 2017-VPC 1, indicating higher green algal, diatom and cyanobacterial abundance with low VPC 1 scores and vice versa. Fluorometrically measured Chlorophyll-a concentrations negatively correlate with 2017-VPC 1 across all sites during 2017 ($r = -0.754$, $p = 0.001$, $n = 36$; Fig. 6a), supporting this correlation and the applicability of this VPC as a proxy for phytoplankton abundance. The second component; 2017-VPC 2 explains 37.8% of the variance and

positively correlates with a mixture of smectite and chlorite (Tables 6-7 and Fig. 4b). Hence this VPC is considered as a proxy for turbidity and suspended material/sediments in the water column. Significant correlations between 2017-VPC 2 and TSS across all sites during 2017 ($r = -0.76$, $p = 0.001$, $n = 60$) confirm the presence of mineral matter (smectite + chlorite) in 2017-VPC-2 (Fig. 6c). The negative correlation between 2017-VPC-2 and TSS implies that higher 2017-VPC 2 scores represent lower turbidity and vice versa. A mixture of goethite, peridinin; a chlorophyll pigment found in dinoflagellates and myxoxanthophyll; a pigment found in the photosynthetic apparatus of cyanobacteria (Tables 6-7 and Fig. 4c) positively correlates with 2017-VPC 3 which explains 9.5 % of the variability of reflectance data. Hence, this VPC is a proxy for suspended goethite, dinoflagellates and cyanobacteria. The fourth component (2017-VPC 4) explains 2.2% of the variance and is a mixture of calcite, Dinophyta and Cyanophyta (Tables 6-7 and Fig. 4d). Calcite positively correlates with VPC4 while Dinophyta (dinoflagellate algae) and Cyanophyta (cyanobacteria) negatively correlate with VPC 4.

Bacillariophyceae (diatoms) contribute to the leading components during both the sampling years (2016-VPC 1 as well as 2017-VPC 1). This observation is consistent with previous observations that diatoms are a dominant group of phytoplankton in OWC (Reeder and Binion, 2008). Cryptophytes contributed to 2016-VPC 2 when the mouth bar was closed but did not contribute to any of the leading VPCs in 2017. This observation is also consistent with Bonini (2013), where cryptophytes were observed only during closed-mouth bar conditions, but not during open-mouth bar conditions. However, 1-3% of the algal cell counts at the site WM consisted of cryptophytes (Crytophyceae). This lower abundance could be a reason why Crytophyceae does not leave a significant spectral signature in 2017 reflectance data. Dinoflagellates were minor constituents during both open and closed-mouth bar conditions, while there weren't any reported from the cell counts. This observation is consistent with the previous observations that the dinoflagellates are not a major component of the estuary (Herdendorf *et al.*, 2004).

Two of the three leading components (VPC 2 and 3) had some aspect of sediment in this turbid water system during both sampling years. However, the compositions of the sediment are significantly different between the two years. Illite makes up much of the suspended sediments during the 2016 sampling period, while it is mainly smectite and chlorite during 2017. The large surface area to depth ratio of the estuary enhances the suspension of bottom sediment with wind-related mixing (Klarer and Millie, 1989). July 2016, is characterized as a period of below-average precipitation (122-year average from 1895-2016, National Oceanic and Atmospheric Administration NOAA; https://www.ncdc.noaa.gov/temp-and-precip/us-maps/). Hence, resuspension of sediment from the illite-dominating estuary floor (Buchanan, 1983) likely contributed to the turbidity. In contrast, during 2017 which is considered a recoremeed wet period https://www.ncdc.noaa.gov/temp-andprecip/us-maps/, smectite and chlorite transported from the upper parts of the OWC watershed make up much of the sediment. Previous work suggests similar changes in constituents determining the optical properties of water as the barrier beach isolates the estuary from Lake Erie (Bonini, 2013; 2016).
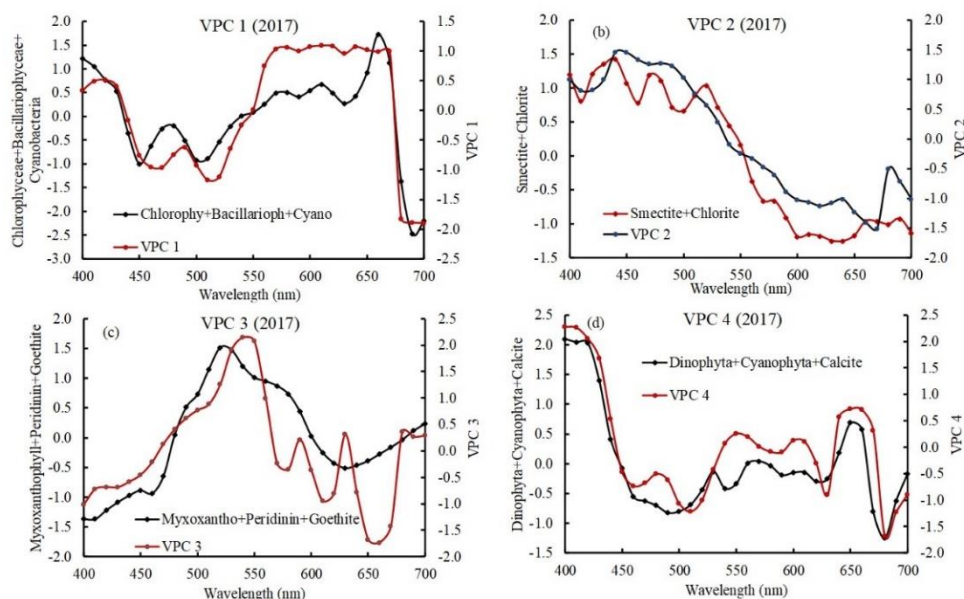

Fig. 4: Comparison of first four principal components of summer 2017 VDS data with their reference spectra. The red line represents the VPCs and the black line represents their reference spectra
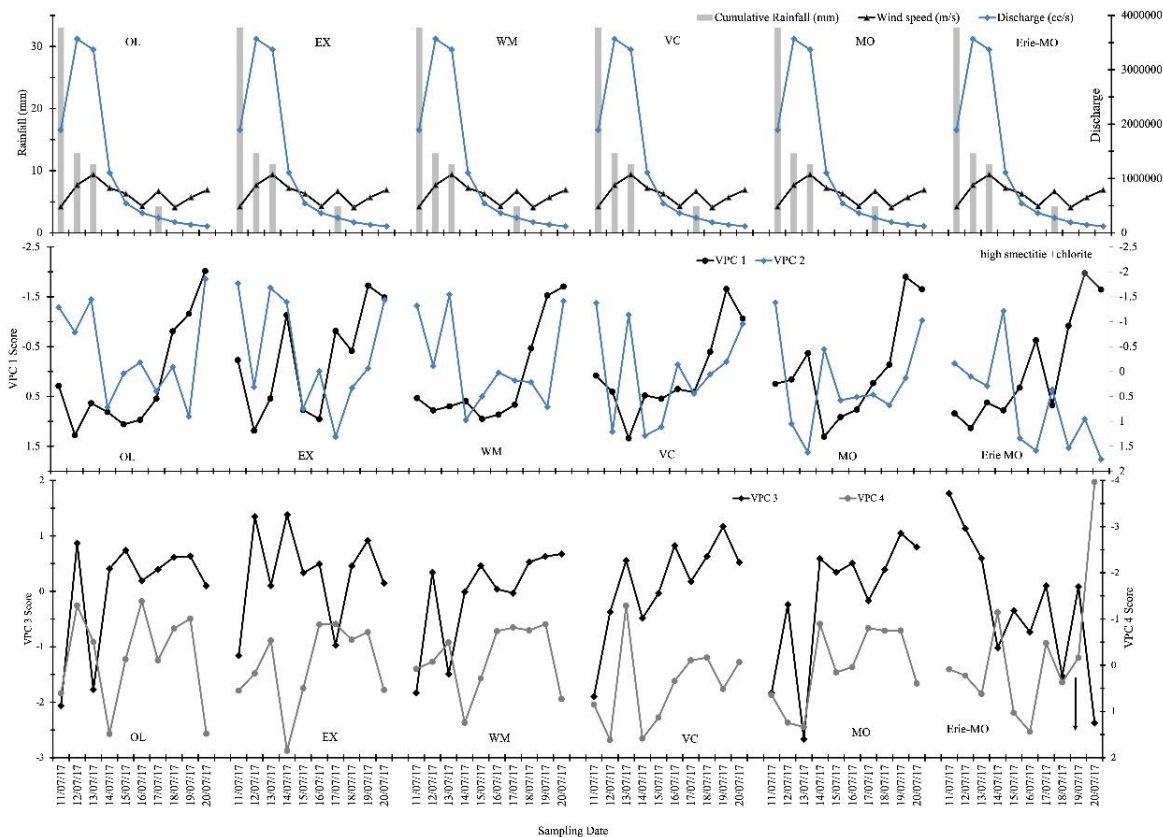
Fig. 5: Temporal variation of VPCs during the 2017 sampling year, the x-axis represents the sampling dates from7/11/17 to 7/20/17, top panel: Black line and triangles-maximum wind speed (m/s) at the time of sampling, gray bars-cumulative daily rainfall (mm), blue diamonds; daily discharge cubic centimeters per second. Middle panel; black line-VPC1, grey line-VPC2. Bottom panel: Black line-VPC 3, grey line- VPC 4, note that the axis of VPC 4 is flipped, hence peaks in gray lines represent low calcite and vice versa
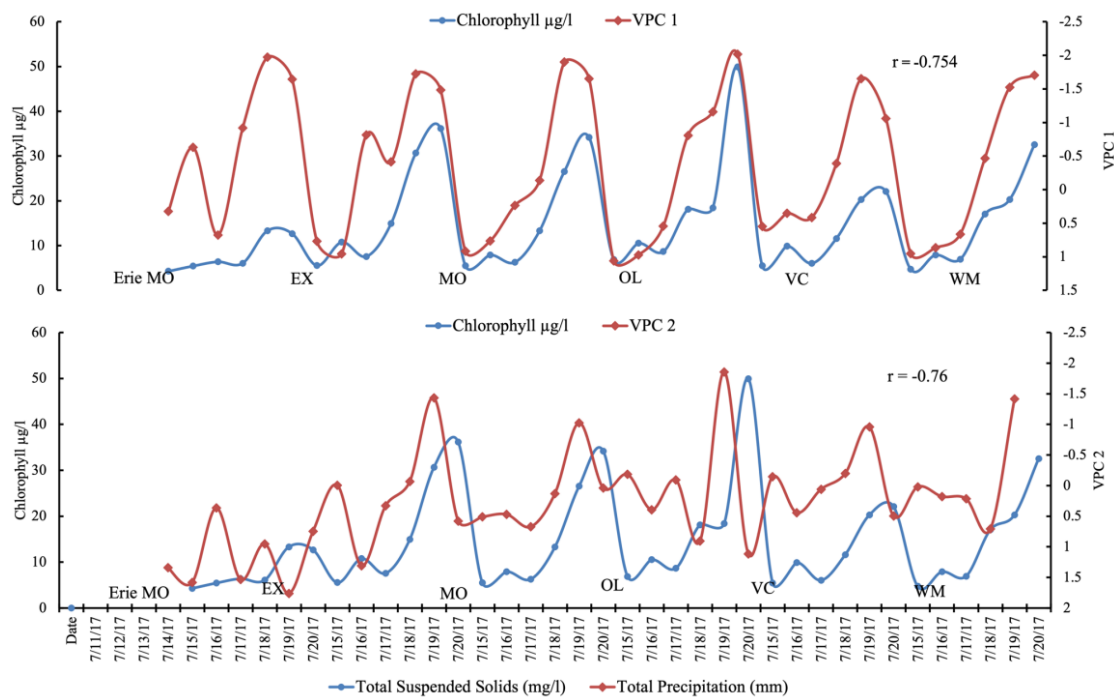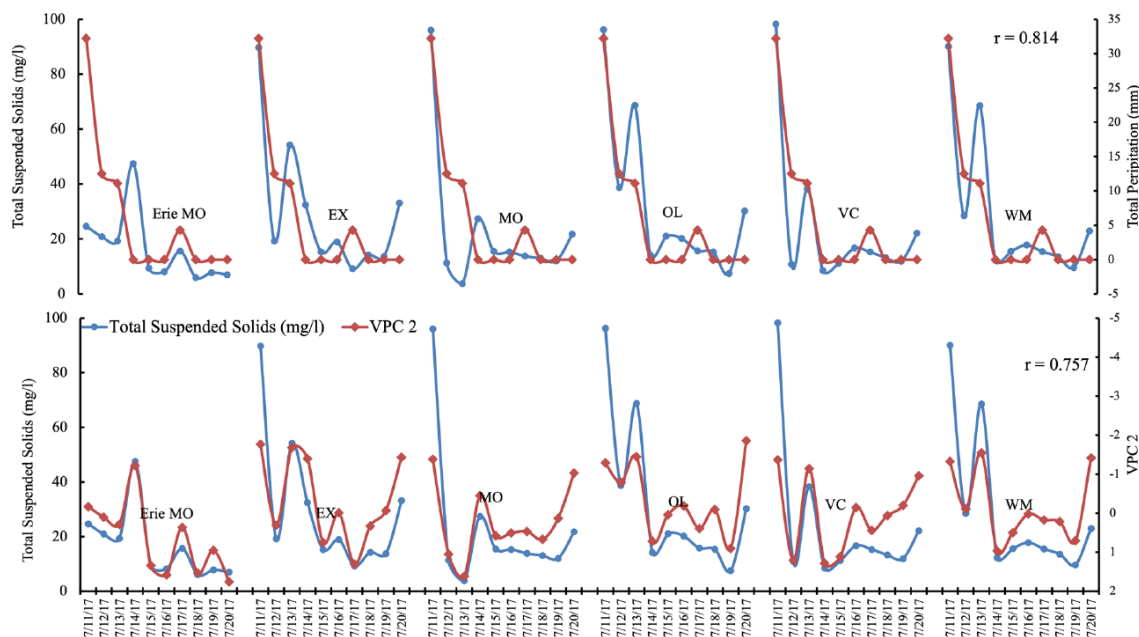
Fig. 6: Time series plots of significantly correlated water quality parameters across the six sampling sites during the year 2017.
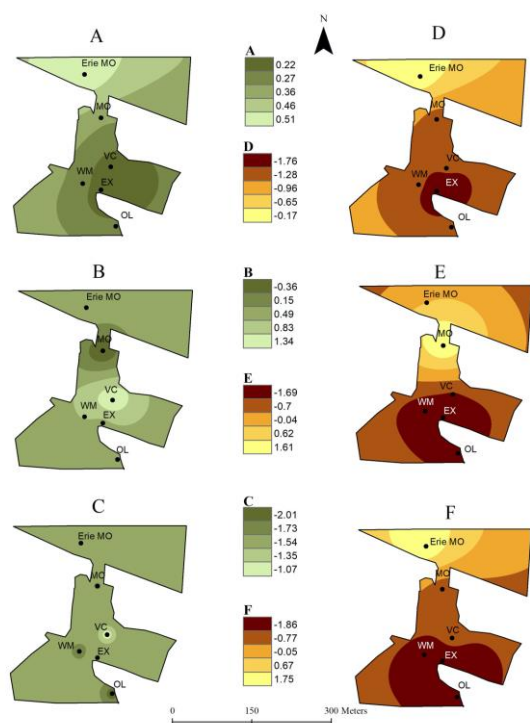

Fig. 7: Spatial variation of VPC 1 (green algae + diatom + cyanobacteria). A-day 1, B-day 3 (after a significant amount of rainfall) and C- day 10 of sampling. Spatial variation of VPC 2 (smectite + chlorite). D-day one, E-day three and F-day 10 of sampling. Notice that the color codes are different for each figure with dark colors representing more phytoplankton/sediment and lighter colors representing less phytoplankton/sediment

Measured percent oxygen levels ($r = 0.53$, $p = 0.001$, $n = 36$) correlate with 2017-VPC 1 across all sites presumably due to the release of oxygen by photosynthesis. This observation confirms the applicability of VPC-1 as a proxy for primary productivity. Despite the higher correlation between dissolved oxygen and 2017-VPC 1 at all other sites, site VC has a lower correlation with VPC 1 ($r = 0.20$, $n = 6$). However, the correlation strengthens when oxygen concentration lagged by a day behind VPC 1 ($r = 0.74$, $p = 0.15$, $n = 5$). This contrasting behavior at VC could be due to the influence of abundant aquatic macrophytes at the site rather than phytoplankton. Emergent aquatic macrophytes can directly alter the dissolved oxygen in the water column through their contribution to photosynthesis (Rose and Crumpton, 1996).

Despite being a mixture of Chlorophyceae, cyanobacteria and Bacillariophyceae pigments, significant correlations were not observed between 2017-VPC 1 and combined relative percentages of the cell counts of Chlorophyceae, cyanobacteria and Bacillariophyceae at four of the five sampling sites. A significant correlation ($r = 0.87$, $p = 0.05$, $n = 5$) was observed only at sites VC between 2017-VPC 1 and percent Bacillariophyceae. Additionally, 2017-VPC 3 correlates with the Chlorophyceae + cyanobacteria + Bacillariophyceae percentages at the site EX ($r = -1$, $p = 0.05$, $n = 5$), where there was a visible growth of an algal bloom.

A general lack of correlation between VPC 1 and cell count percentages from phytoplankton groups consisting of chlorophyll could be associated with

differences in the cell size between different phytoplankton groups. Future studies of the site could benefit from the collection of both taxonomic abundance and biovolume data. However, a lack of correlation between algal volume and chlorophyll concentration had also been reported from previous literature comparing different primary productivity monitoring methods conducted at OWC (Reeder and Binion, 2001). Additionally, counting was terminated as the number of cells from a certain group reached 100, according to the algal cell counting method adopted (Brierley *et al.*, 2007). This approach can eliminate some of the phytoplankton cells present in the sample. An alternative approach would be to count up to 400 cells from the most abundant group, which can significantly increase the analysis time and limit the applicability of the method to larger water bodies and sample numbers. The cell count method uses 1 mL of the collected sample, with the assumption that the sample will provide a representative overview of the cell counts. In contrast, the reflectance approach used here filtered the entire 250 mL of the sample onto a filter paper and the reflectance was measured over four different quadrants of the filter paper. Hence the reflectance signal is rapid and much more representative of the color-producing agents in the water compared to the cell counts.

An increasing trend is demonstrated by 2017-VPC 3 (cyanobacteria + dinoflagellate algae + goethite), at sites MO, OL, WM and VC during the sampling period. Goethite is commonly found associated with Lake Erie sediments (Ortiz *et al.*, 2013) and is considered the dominant iron oxyhydroxide phase in many lake sediments (Van Der Zee *et al.*, 2003). The presence of goethite in this VPC represents iron-rich sediment derived from bog iron ore and peat deposits in the former lagoonal marshes in the central parts of the watershed and/or the erosion of reddish-brown Vaughnsville loam soils (Herdendorf *et al.*, 2004). Total suspended solids strongly correlate with 2017-VPC 3 at sites OL and WM ($r = -0.908$, $p = 0.001$, $n = 20$) suggesting goethite precipitation is concentrated at sites with the greatest accumulation of flow from upstream locations. This observation agrees with the high total iron concentrations that have been recorded during periods of high-water turbidity (Herdendorf *et al.*, 2004). Average iron concentrations as high as 1.86 and 1.12 mg/L had been reported from OWC mouth and nearshore Lake Erie off of OWC in the past (Herdendorf *et al.*, 2004) (Ohio EPA standard for iron is 0.3 mg/L).

Significant correlation between 2017-VPC 3 and ORP at sites OL and WM, further suggests the potential for goethite precipitation at these sites ($r = -0.623$, $p = 0.001$,

$n = 20$; numbers represent the correlation coefficient for the data from both sites combined). The negative correlation between ORP and 2017-VPC 3 suggests higher goethite precipitation under low ORP (oxic conditions), probably resulting from the resuspension of bottom sediment as suggested by Herdendorf *et al.* (2004). Alternatively, goethite precipitation could result from microbial-mediated oxidation of iron (Van De Zee *et al.*, 2003). However, collected water quality data is insufficient to support such precipitation and is beyond the scope of this study.

A decline in 2017-VPC4 is observed at all sites one to two days after a significant amount of rainfall in 2017 (Fig. 5). This component positively correlates with calcite, while negatively correlates with Dinophyta and Cyanophyta. Hence, this decline suggests a decrease in calcite and an increase in cyanobacteria and dinoflagellate abundance. The decline in 2017-VPC 4 with rainfall suggests the dilution of calcite after rainfall. Previous research from the estuary concluded that the concentration of compounds such as calcite entering the estuary through groundwater decreases with the influx of stormwater (Herdendorf *et al.*, 2004; McCarthy *et al.*, 2007). In contrast, the strong correlation between pH and 2017-VPC 4 at site EX ($r = 0.91$, $p = 0.011$, $n = 10$) (SI Fig. 1) could be associated with bio-induced carbonate precipitation by pelagic phytoplankton (Platt and Wright, 1991). EX is a site with extensive phytoplankton overgrowth. Therefore, CO_2 uptake by phytoplankton for photosynthesis can increase the pH of water during times of higher algal productivity (Reeder and Binion, 2001).

A high correlation is observed between stormwater runoff and suspended sediments in the rivers of Northwestern Ohio (McCarthy *et al.*, 2007). This idea is supported by the observed trends and correlations between principal components containing sediment during both the sampling years at OWC. Total suspended solids were highest at the beginning of the sampling period in all sites except at Erie-MO in 2017. Whereas at the Erie-MO site, the highest TSS and VPC 2 levels are recorded on the fourth day of the sampling. This observation is also supported by the statistically significant correlation between precipitation and TSS at these five sites ($r = 0.87$, $p<0.001$, $n = 60$). A significant correlation is observed between the precipitation and TSS at Erie-MO ($r = 0.68$, $p = 0.04$, $n = 10$) when TSS lagged behind precipitation by three days (SI Fig. 2). This increase in TSS a few days after the rainfall represents the lag time associated with the arrival of suspended material from the upper parts of the watershed to the lake. Additionally, the increase in turbidity could also be associated with the resuspension

of bottom sediments due to the higher wind speeds associated with the storm events (Fig. 5). During 2016, VPC 1 declined one to two days following the storm events. This decline suggests a decline in illite (clay component of VPC1), rather than a decline in diatoms; confirming a decrease in turbidity within the estuary as stormwater recedes. Observed temporal trends and correlations between stormwater input and suspended sediment loads at OWC are consistent with previous research that the concentration of insoluble sediments increases with the input of surface runoff (Herdendorf *et al*., 2004; McCarthy *et al*., 2007; Bonini, 2013; 2016). In summary, temporal trends of TSS and 2017-VPC 2 closely follow the 24 h cumulative rainfall, confirming the inflow of sediment-laden runoff to the estuary from the watershed.

Storm runoff events carrying nutrients into the estuary are considered a key factor controlling the phytoplankton abundance in the OWC estuary (Van De Zee *et al*., 2003; Herdendorf *et al*., 2004; Bonini, 2016). In contrast to the rapid increase in turbidity; green algae, diatoms and cyanobacteria represented by 2017-VPC 1 declined one to two days after the storm events at all sites with the lowest decline at EX. This decline could be associated with the turbidity created by the stormwater and the flushing of phytoplankton down the estuary (McCarthy *et al*., 2007). Previous work suggested that the water retention time at the estuary is approximately a day, hence a decline in phytoplankton 2-3 days after a storm event is expectable. It is possible that site EX, which has limited water circulation, is protected from stormflow, creating a refuge for phytoplankton during storm events or allowing the buildup of material transported from other sites to this zone of low water flow. However, 2017-VPC 1 and chlorophyll concentrations increased two to three days after the storm events. This could be related to the rapid repopulation of the lower estuary following the storm events. Klarer and Millie (1994) reported a similar decline in phytoplankton abundance with increasing stormflow at the lower estuary, but it rapidly increased four-fold, approximately four days after the storm event.

Nonetheless, it is hard to evaluate the influence of a single storm event on the phytoplankton abundance as there had been scattered storms throughout the sampling period (Fig. 5). The observed increase in phytoplankton could also be associated with the estuary environment being stabilized, allowing more chlorophyll *a*-producing algae to flourish. However, such a prominent decline in phytoplankton abundance was not observed immediately after the storm events during 2016 (VPCs 2 and 3; Fig. 3). However, green algae and cyanobacteria (2016-VPC 2) increased one to two days after the storm events during 2016, possibly due to the flushing of phytoplankton from

the upper estuary and increased availability of nutrients from sediment resuspension (Klarer and Millie, 1994) (Fig. 5). This difference in phytoplankton behavior could be associated with the conditions of the mouth bar, as well as meteorological conditions and nutrient sources. When the mouth bar is open, stormwater can flush phytoplankton out from the estuary into the lake basin resulting in an immediate decline after storm events. In contrast, when the mouth bar is closed, phytoplankton would accumulate within the estuary. This comparison supports the idea that there is a higher physical instability within the estuary and the phytoplankton responds to physical processes rather than biological processes when the mouth bar is open (Herdendorf *et al*., 2004).

The maps showing the surface distribution of 2017-VPC 1 and 2 (smectite and chlorite) further support the idea of transportation of algae and sediment across the estuary during the ten-day sampling period for the year 2017 (Fig. 7). It is clear that phytoplankton (green algae, diatoms and cyanobacteria) were less abundant and were concentrated in the four upstream locations (Fig. 7A), while the sediments were more abundant and were evenly distributed throughout the estuary on the first day of sampling, which was after a significant amount of rainfall (32.2 mm within 24 h; Figs. 7. A and D). Sediments were more concentrated in the upper part of the estuary by the third day of sampling as the storm runoff retreated. In contrast, phytoplankton were more concentrated around the mouth-bar (Figs. 7B and 7E). Algae, diatoms and cyanobacteria were dispersed throughout the estuary but more accumulated around the mouth bar by the tenth day as the mouth bar progressively closed. Sediments were accumulated by the mouth bar and the concentration was higher in the three upstream sampling sites (WM, EX and OL) with less sediment in the lake, supporting a limited passage of sediment into the lake through the narrowing of the mouth bar, by the tenth day.

Flow from OWC to Lake Erie decreased as the mouth bar started to close, by the end of the 2017 sampling period. The inhibited flow to Lake Erie caused 2017-VPC 2 to increase upstream of the mouth bar and decreased on the lakeside of the mouth bar (Erie-MO) as a result of accumulating estuary sediment, due to a bottleneck effect created by the narrow mouth bar (Fig. 7). Herdendorf *et al*. (2004) noted a fourfold decrease in specific conductivity of the estuary water when it mixes with Lake Erie water. Hence this increase in 2017-VPC 2 at the estuary mouth suggest less mixing of estuary water with the lake water as the mouth bar closes. These trends observed in 2017-VPC 2 and VPC 1 suggest that the mouth bar regulates the transportation of clay minerals from the estuary to Lake Erie (Fig. 7B). Decreasing trends, demonstrated by all four 2017-VPCs at the Erie-MO site on the final day of sampling further confirms the idea of the limited passage

of phytoplankton and sediment into Lake Erie through the OWC estuary when the mouth bar is closed. Observed temporal variations in 2017-VPCs demonstrate the transportation of sediment and phytoplankton through the open mouth bar into Lake Erie and the accumulation of these materials at upstream sampling sites as the mouth bar progressively closed. In contrast to the observed spatial variability of 2017-VPCs 1 and 2 (Fig. 7), the surface distribution of 2016-VPC 1 and 2 do not show significant trends, hence not included here.

Chlorophyll concentration and 2017-VPC 1 scores (which reflect green algae, diatoms and cyanobacteria abundance) have an overall increasing trend in all sampling sites within the estuary as the mouth bar closes (Fig. 5, middle panel). This observation is in contrast to a prior observed decline in net primary productivity at site WM during the closing of the mouth bar (Bonini, 2016). However, the net primary productivity model of Bonini (2016) is based on multiyear diurnal variability of pH and dissolved oxygen. Dissolved oxygen concentration in aquatic ecosystems can be affected by photosynthesis, respiration as well as meteorological factors like wind-related mixing. Hence contrasting results can be expected, when comparing diurnal water quality-based net primary productivity quantifications with pigment-based quantifications. Additionally, the (Bonini, 2016) model was based on the site WM, while this study is based on five additional sampling sites, (two upstream from WM and three downstream from WM) over a much shorter timescale. Hence the differences in hydrological properties at different sampling sites can lead to contrasting results.

Strong correlations exist between all four leading 2017-VPCs at OL and WM (r = 0.918, p = 0.001, n = 80) suggesting similar phytoplankton and sediment composition at these two sites during 2017. This observation supports the idea that sediment and algae are transported across the estuary (SI Fig. 3). However, such a correlation does not exist between the two sites during the previous year (r = 0.22, n = 66). Diatom and illite abundances (reflected by 2016VPC 1) were higher in the two upstream sampling sites; OL and WM and demonstrate progressive increase towards the Mouth bar (MO). It is possible that the closed mouth bar acted as a barrier for the dispersal of estuary sediments and diatoms into Lake Erie. Observed differences between the two sampling years would have resulted from the changes in hydrological conditions, nutrient availability, meteorological conditions and/or zooplankton variability between the two sampling years. July 2016 is considered a relatively dry year (much below average precipitation), while July 2017 is considered a record wet year compared to the 1895-2016 average precipitation according to the

NOAA (https://www.ncdc.noaa.gov/temp-and-precip/us-maps). Consistent with this observation, the OWC received a total of 69.1 mm of rainfall during the ten-day sampling period in 2017. This was a 61% increase compared to the relatively dry 2016 sampling period (26.5 mm). Prior studies suggest that increased precipitation together with quiet water conditions can lead to record-breaking blooms similar to the 2011 Lake Erie bloom (Michalak *et al*., 2013). Under changing climatic conditions precipitation in the Midwest is expected to increase, with events >20 mm increasing by 50% (Michalak *et al*., 2013). Higher runoff associated with increased precipitation can lead to higher sediment yield in waterbodies. Similarly, high inflow events can greatly affect sediment transportation across the estuary into Lake Erie. A comparison of 2016 and 2017 data further supports the idea that the risk of algal blooms can increase with episodic increases in nutrient loading associated with storm events. Hence sediment and algal bloom mapping presented in our work can be useful in evaluating the health of aquatic water bodies as this method is rapid and cost-effective compared to other algal bloom monitoring methods. The other advantage of VDS over other methods is its ability to identify the sediment composition in water bodies.

Conclusion

Principal component analysis of visible derivative spectroscopic data during the relatively dry 2016 sampling period yielded three components explaining 95% of the variance of the data, including diatoms + clay, cyanobacteria + dinoflagellate algae/clay and cyanobacteria + green algae. Four VPCs explained 99% of the variance in VDS data during the summer of 2017, all of which consist of cyanobacteria and suspended sediments. The leading component (VPC 1) during the record wet 2017, under open-mouth bar conditions, consisted of diatoms, cyanobacteria and green algae, while the second component (VPC 2) entirely consisted of suspended clay. Considerable difference in sediment composition is observed between the two sampling years with illite deriving from the suspension of estuary sediments dominating during 2016; while smectite, chlorite and goethite derived from the upper parts of the OWC watershed dominated during the relatively wet 2017. Significant correlation between VPC 1 versus chlorophyll a and VPC 2 versus TSS, from 2017 data supports the successful applicability of reflectance spectroscopy to monitor phytoplankton and sediment assemblages at OWC. Observed phytoplankton pigment combinations observed at OWC are consistent with previous research based on algal cell counts confirming the applicability of this method. Comparison between VPCs and weather data suggests that stormwater causes a significant impact on the estuary phytoplankton abundance. Diatom, cyanobacteria and

green algae abundance declined immediately after storm events throughout the lower estuary when the mouth bar is open, except at site EX where water circulation is limited. In contrast, a significant decline is not observed when the mouth bar is closed, suggesting flushing of phytoplankton through the estuary into the lake when the mouth bar is open. An increase in all types of phytoplankton is observed 2-3 days after storm events when the mouth bar is open and closed, due to the availability of nutrients transported downstream associated with stormwater. Prepared surface distribution maps of 2017-VPC 1 supports the idea of transportation of phytoplankton across the estuary into the Lake Erie. Phytoplankon were accumulated around the mouth bar as it started to progressively narrow by the end of the sampling period, confirming that OWC serves as a source of phytoplankton to the estuary. Simulataneous with the closing of the mouth bar, sediment load declined along the nearshore of Lake Erie, but increased at the upstream sampling sites, confirming the ecological significance of the estuary as a sediment sink.

Our results support the applicability of VDS methods in the qualitative identification of phytoplankton groups in large water bodies. The results further demonstrate the strengths of VDS methods in mapping sediment and algal bloom distribution in waterbodies. Additionally, VDS methods can help us understand the composition of suspended sediments which is necessary for identifying sediment sources when implementing sediment control strategies, which would be vital under changing climatic conditions that can lead to stronger storm events bringing in more sediment to waterbodies.

Acknowledgment

Funding Information

Author's Contributions

Lorita Nivanthi Mihindukulasooriya: Designed the project, conducted fieldwork, analyzed the data and wrote the manuscript.

Brenna Shae Mabry: Conducted fieldwork and sample collection during the 2017 field season, analyzed data and was involved in writing some parts of the manuscript.

Madison Slocum: Conducted the algal cell counts.

Joseph Daniel Ortiz: Guided field sampling in 2016 and provided assistance with data interpretation and manuscript preparation.

Ethics

This material is the authors' own original work, which has not been previously published elsewhere.

Competing Interests

The authors declare that they have no competing interests.

References

Avouris, D. M., & Ortiz, J. D. (2019). Validation of 2015 Lake Erie MODIS image spectral decomposition using visible derivative spectroscopy and field campaign data. *Journal of Great Lakes Research*, *45*(3), 466-479.
https://doi.org/10.1016/j.jglr.2019.02.005

Bernal, B., & Mitsch, W. J. (2008). A comparison of soil carbon pools and profiles in wetlands in Costa Rica and Ohio. *Ecological Engineering*, *34*(4), 311-323.
https://doi.org/10.1016/j.ecoleng.2008.09.005

Bonini, N. (2013). *Comparison of VNIR Derivative and Visible Fluorescence Spectroscopy Methods for Pigment Estimation in an Estuarine Ecosystem: Old Woman Creek*. Kent State University.
http://rave.ohiolink.edu/etdc/view?acc_num=kent1382838748

Bonini, N. (2016). *Assessing the Variability of Phytoplankton Assemblages in Old Woman Creek* (1-). Kent State University.
http://rave.ohiolink.edu/etdc/view?acc_num=kent1469959717

Bouchard, F., Pienitz, R., Ortiz, J. D., Francus, P., & Laurion, I. (2013). Palaeolimnological conditions inferred from fossil diatom assemblages and derivative spectral properties of sediments in thermokarst ponds of subarctic. *Boreas*, *42*, 575-595.
https://doi.org/10.1111/bor.12000

Brierley, B., Carvalho, L., Davies, S., & Krokowski, J. (2007). *Guidance on the quantitative analysis of phytoplankton in Freshwater Samples*. Report to SNIFFER (Project WFD80).
https://nora.nerc.ac.uk/id/eprint/5654/1/Phytoplankton_Counting_Guidance_v1_2007_12_05.pdf

Buchanan, D. B. (1983). *Transport and Deposition of Sediment in Old Woman Creek Estuary of Lake Erie*.
https://repository.library.noaa.gov/view/noaa/42923/noaa_42923_DS1.pdfd

Clark, R. N., Swayze, G. A., Wise, R. A., Hoefen, T. M., Kokaly, R. F., & Sutley, S. J. (2007). [dataset]. In *USGS digital spectral library splib06a (No. 231). US Geological Survey.*
https://doi.org/10.3133/ds231

Kokaly, R. F., Clark, R. N., Swayze, G. A., Livo, K. E., Hoefen, T. M., Pearson, N. C., Klein, A. J., Wise, R. A., Benzel, W., Lowers, H. A., & Driscoll, R. L. (2017). USGS Spectral Library Version 7 [dataset]. *In USGS Publications warehouse*.
https://doi.org/10.3133/ds1035

Evans, J. E., & Seamon, D. E. (1997). A GIS Model to Calculate Sediment Yields from a Small Rural Watershed, Old Woman Creek, Erie and Huron Counties. *Ohio Journal of Science*, *97*(3), 44-52.
http://hdl.handle.net/1811/23743

Shear, H., & Wittig, J. (1995). The Great Lakes: An environmental atlas and resource book (Chpter 2. In K. Fuller (Ed.), *Natural Resources and the Environment* (3, Illustrated, Reprint, Vol. *95*, p. 46). Great Lakes National Program Office, U.S. Environmental Protection Agency, 1995.
ISBN-10: 9780662234418.

Gordon, H. R., Brown, O. B., & Jacobs, M. M. (1975). Computed Relationships Between the Inherent and Apparent Optical Properties of a Flat Homogeneous Ocean. *Applied Optics*, *14*(2), 417-427.
https://doi.org/10.1364/ao.14.000417

Gordon, H. R., Brown, O. B., Evans, R. H., Brown, J. W., Smith, R. C., Baker, K. S., & Clark, D. K. (1988). A semianalytic radiance model of ocean color. *Journal of Geophysical Research: Atmospheres*, *93*(D9), 10909-10924.
https://doi.org/10.1029/jd093id09p10909

Han, L. (2005). Estimating chlorophyll-a concentration using first-derivative spectra in coastal water. *International Journal of Remote Sensing*, *26*(23), 5235-5244.
https://doi.org/10.1080/01431160500219133

Herdendorf, C. E., Klarer, D. M., & Herdendorf, R. C. (2004). *The Ecology of Old Woman Creek, Ohio: An Estuarine and Watershed Profile* (1-).
https://dam.assets.ohio.gov/image/upload/ohiodnr.gov/documents/coastal/owc/Profile2nd_FrontMaterial.pdf

Klarer, D. (1988). *The Role of a Fresh Water Estuary in Mitigating Storm Water Inflow (OWC Technical report)* (1-). Ohio Department of Natural Resources.
https://www.amazon.com/Estuary-Mitigating-Inflow-Technical-report/dp/B00072UPKQ

Klarer, D. M., & Millie, D. F. (1989). Amelioration of storm-water quality by a freshwater estuary. *Archiv für Hydrobiologie*, *116*(3), 375-389.
https://doi.org/10.1127/archiv-hydrobiol/116/1989/375

Klarer, D. M., & Millie, D. F. (1994). Regulation of phytoplankton dynamics in a Laurentian Great Lakes estuary. *Hydrobiologia*, *286*(2), 97-108.
https://doi.org/10.1007/bf00008500

Lemasson, C., Marsac, N. T. D., & Cohen-Bazire, G. (1973). Role of Allophycocyanin as Light-Harvesting Pigment in Cyanobacteria. *Biological Sciences*, *70*(11), 3130-3133.
https://doi.org/10.1073/pnas.70.11.3130

McCarthy, M. J., Gardner, W. S., Lavrentyev, P. J., Moats, K. M., Jochem, F. J., & Klarer, D. M. (2007). Effects of Hydrological Flow Regime on Sediment-water Interface and Water Column Nitrogen Dynamics in a Great Lakes Coastal Wetland (Old Woman Creek, Lake Erie). *Journal of Great Lakes Research*, *33*(1), 219-231.
https://doi.org/10.3394/0380-1330(2007)33[219:eohfro]2.0.co;2

Michalak, A. M., Anderson, E. J., Beletsky, D., Boland, S., Bosch, N. S., Bridgeman, T. B., Chaffin, J. D., Cho, K., Confesor, R., Daloğlu, I., DePinto, J. V., Evans, M. A., Fahnenstiel, G. L., He, L., Ho, J. C., Jenkins, L., Johengen, T. H., Kuo, K. C., LaPorte, E., … Zagorski, M. A. (2013). Record-setting algal bloom in Lake Erie caused by agricultural and meteorological trends consistent with expected future conditions. *Biological Sciences*, *110*(16), 6448-6452.
https://doi.org/10.1073/pnas.1216006110

Mihindukulasooriya, L. N., Ortiz, J. D., Pompeani, D. P., Steinman, B. A., & Abbott, M. B. (2015). Reconstruction of late Quaternary paleohydrologic Conditions in southeastern British Columbia using visible derivative spectroscopy of Cleland Lake Sediment. *Quaternary Research*, *83*(3), 531-544.
https://doi.org/10.1016/j.yqres.2015.02.003

Mitsch, W. J., & Reeder, B. C. (1992). Nutrient and hydrologic budgets of a great Lakes coastal freshwater wetland during a drought year. *Wetlands Ecology and Management*, *1*, 211-222.
https://doi.org/10.1007/bf00244926

Ortiz, J. D. (2011). Application of Visible/near Infrared derivative spectroscopy to Arctic paleoceanography. *IOP Conference Series: Earth and Environmental Science*, *14*, 012011.
https://doi.org/10.1088/1755-1315/14/1/012011

Ortiz, J. D., Avouris, D., Schiller, S., Luvall, J. C., Lekki, J. D., Tokars, R. P., Anderson, R. C., Shuchman, R., Sayers, M., & Becker, R. (2017). Intercomparison of Approaches to the Empirical Line Method for Vicarious Hyperspectral Reflectance Calibration. *Frontiers in Marine Science*, *4*, 00296. https://doi.org/10.3389/fmars.2017.00296

Ortiz, J. D., Avouris, D. M., Schiller, S. J., Luvall, J. C., Lekki, J. D., Tokars, R. P., Anderson, R. C., Shuchman, R., Sayers, M., & Becker, R. (2019). Evaluating visible derivative spectroscopy by varimax-rotated, principal component analysis of aerial hyperspectral images from the western basin of Lake Erie. *Journal of Great Lakes Research*, *45*(3), 522-535. https://doi.org/10.1016/j.jglr.2019.03.005

Ortiz, J. D., Polyak, L., Grebmeier, J. M., Darby, D., Eberl, D. D., Naidu, S., & Nof, D. (2009). Provenance of Holocene sediment on the Chukchi-Alaskan margin based on combined diffuse spectral reflectance and quantitative X-Ray Diffraction analysis. *Global and Planetary Change*, *68*(1-2), 73-84. https://doi.org/10.1016/j.gloplacha.2009.03.020

Ortiz, J. D., Witter, D. L., Ali, K. A., Fela, N., Duff, M., & Mills, L. (2013). Evaluating multiple colour-producing agents in Case II waters from Lake Erie. *International Journal of Remote Sensing*, *34*(24), 8854-8880. https://doi.org/10.1080/01431161.2013.853892

Platt, N. H., & Wright, V. P. (1991). Lacustrine carbonates: facies models, facies distributions and hydrocarbon aspects. *In Lacustrine Facies Analysis* (1-, pp. 57-74). https://doi.org/10.1002/9781444303919.ch3

Reeder, B. C., & Binion, B. M. (2001). Comparison of methods to assess water column primary production in wetlands. *Ecological Engineering*, *17*(4), 445-449. https://doi.org/10.1016/s0925-8574(00)00135-x

Reeder, B. C., & Binion, B. M. (2008). *Algal Community Habitat Preferences in Old Woman Creek Wetland, Erie County, Ohio* (1-). http://hdl.handle.net/1811/48454

Rose, C., & Crumpton, W. G. (1996). Effects of emergent macrophytes on dissolved oxygen dynamics in a prairie pothole wetland. *Wetlands*, *16*(4), 495-502. https://doi.org/10.1007/bf03161339

Stumpf, R. P., Wynne, T. T., Baker, D. B., & Fahnenstiel, G. L. (2012). Interannual Variability of Cyanobacterial Blooms in Lake Erie. *PLoS ONE*, *7*(8), e42444. https://doi.org/10.1371/journal.pone.0042444

USGS. (2017). *USGS surface-water daily data for the nation*. National Water Information System: Web Interface. https://waterdata.usgs.gov/nwis/dv/?referred_m%20 module%20=%20sw

Van Der Zee, C., Roberts, D. R., Rancourt, D. G., & Slomp, C. P. (2003). Nanogoethite is the dominant reactive oxyhydroxide phase in lake and marine sediments. *Geology*, *31*(11), 993. https://doi.org/10.1130/g19924.1

Wijekoon, N. (2007). *Spatial and temporal variability of surface cover in an estuarine ecosystem from satellite imagery and field observations* (1-). Kent State University. http://rave.ohiolink.edu/etdc/view?acc_num=kent11 94621824

Walling, D. E. (2013). The evolution of sediment source fingerprinting investigations in fluvial systems. *Journal of Soils and Sediments*, *13*(10), 1658-1675. https://doi.org/10.1007/s11368-013-0767-2
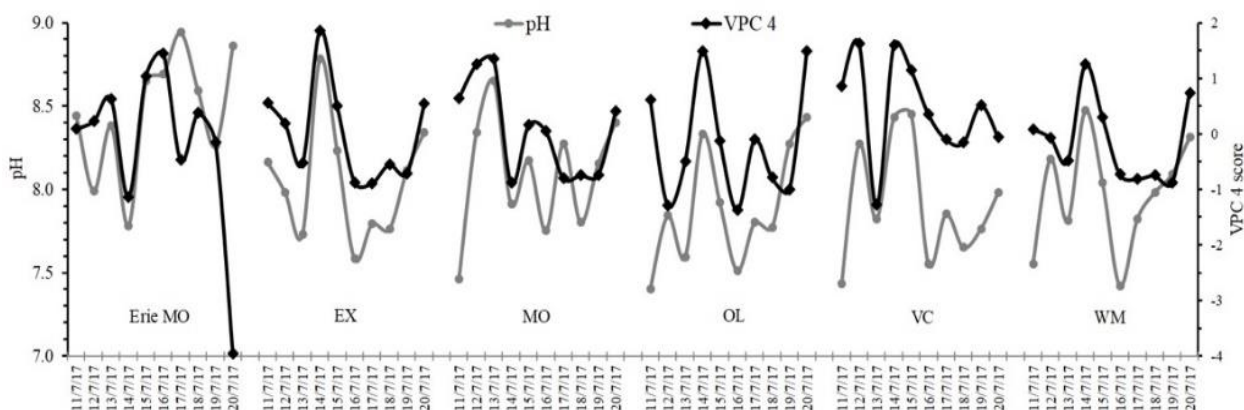
SI Fig. 1: Variation of VPC 4 (black line and circles) and pH (gray line and circles) during the sampling period
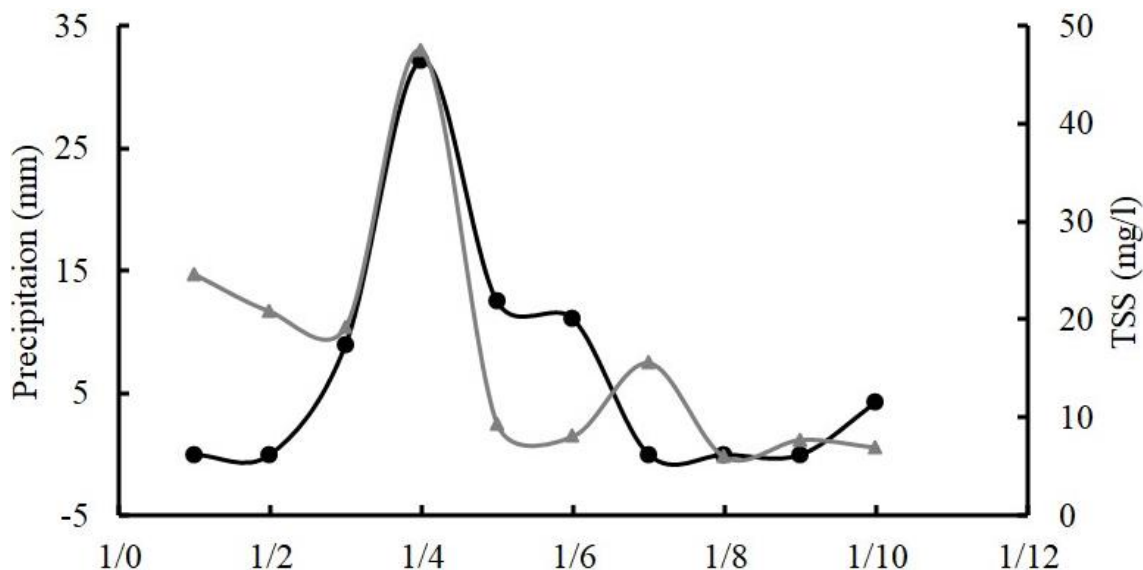
SI Fig. 2: Precipitation (lagged by three days; black line and circles) correlates with TSS (gray line and triangles) at the Erie-MO site when the precipitation is lagged by three days
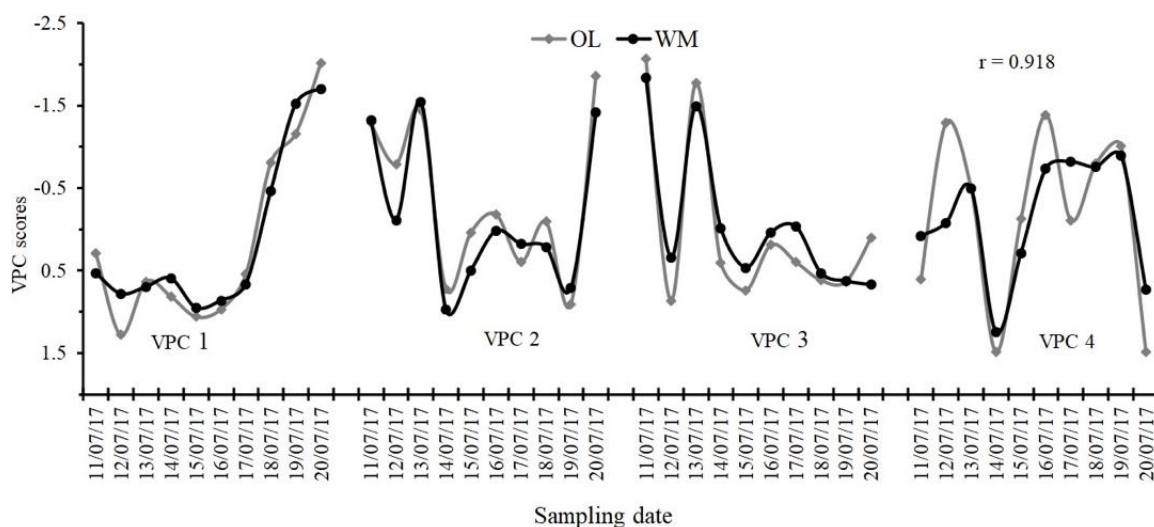
SI Fig. 3: All four PCs for 2017 significantly correlate with each other between the sampling site WM (black line and circle) and OL (gray line and diamonds) suggesting transportation of phytoplankton and sediments across the estuary

SI Table 1: Significant correlations observed between water quality parameters and their significant levels during the two sampling years

Factors	Correlation (r)	Probability (p)	Number of observations (n)
2016			
VPC 1 vs. TSS (mg/L)	-0.69	0.001	40
VPC 2 vs. Max wind Spd (m/s)	0.31	0.050	44
VPC 2 vs. Precipitation (mm)	0.29	0.030	44
VPC 3 vs. Max wind Spd (m/s)	0.32	0.040	44
VPC 3 vs. Precipitation (mm)	-0.24	0.020	44
VPC 3 (1 day lag) vs. Ppt (mm)	-0.38	0.010	44
2017			
VPC 1 vs. DO (%)	0.53	0.001	36
VPC 1 vs. DO (mg/L)	0.46	0.005	36
VPC 1 vs. DO (%) (1 day lag, at VC)	0.74	0.150	5
VPC 1 vs. Chl (µg/L)	0.75	<0.001	36

SI Table 1: Continue

VPC 1 vs. Chl (µg/L) at OL	0.86	0.030	6
VPC 1 vs. Chl (µg/L) at WM	0.94	0.005	6
VPC 1 vs. Chl (µg/L) at VC	0.94	0.005	6
VPC 1 vs. Chl (µg/L) at EX	0.79	0.060	6
VPC 1 vs. Chl (µg/L) at MO	0.94	0.005	6
VPC 1 vs. Chl (µg/L) at Erie-MO	0.82	0.050	6
VPC 2 vs. Chl (µg/L)	0.75	<0.001	36
VPC 2 vs. TSS (mg/L)	0.76	<0.001	60
VPC 2 vs. Max Wind Spd (m/s)	0.24	0.070	60
VPC 3 vs. TSS (mg/L)	-0.50	<0.001	60
VPC 4 vs. pH	0.28	0.030	60
VPC 4 vs. Precipitation (mm) (3 day lag)	0.36	<0.010	50
TSS vs. Chl (µg/L) 0.76	0.61	<0.001	36
TSS vs. Ppt (mm)	0.78	<<0.000.001	60
TSS vs. Pppt (mm) (3 day lag, at Erie-MO)	0.68	0.040	10
VPCs at OL vs. WM	0.92	<0.001	80

SI Table 2: Relative percentages of phytoplankton from the five sampling sites, WM, MO, EX, VC and OL, between 11/07/17 to 15/07/17. A-% Chlorophyceae, B- % Bacillariophycea, C- % Cyanobacteria, D- % Euglenophyceae, E- % Cryptophyta

Sample number and date	A	B	C	D	E
Owc-wm-11/07/17	5.93	3.70	74.07	12.59	3.70
Owc-wm-12/07/17	2.52	5.04	84.03	8.40	0.00
Owc-wm-13/07/17	2.68	6.25	89.29	0.00	1.79
Owc-wm-14/07/17	2.68	4.46	89.29	3.57	0.00
Owc-wm-15/07/17	5.26	4.39	87.72	1.75	0.88
OWC-MO-11/07/17	0.95	1.90	95.24	1.90	0.00
OWC-MO-12/07/17	2.88	0.96	96.15	0.00	0.00
OWC-MO-13/07/17	0.94	0.94	94.34	2.83	0.94
OWC-MO-14/07/17	1.90	0.95	95.24	1.90	0.00
OWC-MO-15/07/17	0.00	1.94	97.09	0.97	0.00
OWC-EX-11/07/17	1.92	0.96	96.15	0.96	0.00
OWC-EX-12/07/17	2.70	3.60	90.09	3.60	0.00
OWC-EX-13/07/17	0.00	1.92	96.15	1.92	0.00
OWC-EX-14/07/17	2.73	2.73	90.91	3.64	0.00
OWC-EX-15/07/17	0.00	0.00	98.04	1.96	0.00
OWC-VC-11/07/17	1.92	0.00	96.15	1.92	0.00
OWC-VC-12/07/17	1.94	0.00	97.09	0.97	0.00
OWC-VC-13/07/17	2.80	1.87	93.46	1.87	0.00
OWC-VC-14/07/17	2.78	1.85	92.59	2.78	0.00
OWC-VC-15/07/17	0.00	0.96	96.15	2.88	0.00
OWC-OL-11/07/17	3.74	0.93	93.46	1.87	0.00
OWC-OL-12/07/17	2.70	3.60	90.09	3.60	0.00
OWC-OL-13/07/17	1.82	2.73	90.91	4.55	0.00
OWC-OL-14/07/17	0.00	2.83	94.34	2.83	0.00
OWC-OL-15/07/17	1.89	1.89	94.34	1.89	0.00